ASSOCIAZIONE NAZIONALE ITALIANA DI INGEGNERIA SISMICA
ANIDIS
Italian National Association of Earthquake Engineering

XVIII CONVEGNO ANIDIS
L'ingegneria sismica in Italia
ASCOLI PICENO 2019
15-19 Settembre

Numerical modelling of column failure due to the local shear interaction in infilled RC frames

Maria Teresa De Risi[a(*)], Carlo Del Gaudio[a], Paolo Ricci[a], Gerardo Mario Verderame[a]
[a]*Università degli Studi di Napoli Federico II - Dipartimento di Strutture per l'Ingegneria e l'Architettura, Via Claudio, 21, 80125, Napoli, Italy*
[(*)]*beneficiary of an AXA Research Fund Post-Doctoral Grant*

Keywords: masonry infills; reinforced concrete frames; local interaction; column shear failure; numerical simulations.

ABSTRACT
The presence of masonry infills in Reinforced Concrete (RC) frames leads to the increase in their lateral strength and stiffness. Nevertheless, post-earthquake observed damage showed that infills can also cause potential brittle failures due to the local interaction with structural elements, thus producing a limitation of deformation capacity of the surrounding frame. A proper numerical model both for infills and RC members is necessary to reliably detect the shear failure of columns due to the local interaction with the masonry infill. Several researches dealt with this topic, by using the equivalent strut model or more complex models like the double- and triple-strut models or FEM-approaches. Nevertheless, the choice of the proper modelling strategies and degrading shear strength model is still a frontier issue for the most recent research works. This paper presents a preliminary numerical investigation on column shear failure due to the local interaction with masonry infills, starting from the results of some experimental tests on infilled frames presented in the literature, which exhibited this kind of failure. Different shear strength models and different strategies of macro-modeling for infills are applied to numerically reproduce the column shear failure and the global response. The modeling strategies are lastly compared with the experimental results to provide a support towards the choice of the most reliable numerical approach.

1 INTRODUCTION

Numerical and experimental studies highlighted that the presence of masonry infills in Reinforced Concrete (RC) frames leads to the increase in their lateral strength and stiffness. Nevertheless, infills can also cause potential brittle failures due to the local interaction with structural elements, thus limiting the deformation capacity of the RC frame. This detrimental effect is particularly important for existing masonry-infilled RC buildings designed for gravity loads only without any capacity design requirements.

During last decades, several experimental studies investigated the seismic behaviour of RC frames with infills, but a few of them investigated the effects of the interaction between the infill panel and surrounding elements resulting in brittle failure mechanisms such as shear failure in RC columns (e.g., Mehrabi et al. 1996; Al Chaar et al. 2002), above all for infills made up of hollow clay bricks, very widespread in the Mediterranean region. The topic certainly deserves a deeper investigation, both about (i) the best infill modelling strategy and, consequently, the definition of the column shear demand due to the interaction, and (ii) the proper shear strength model to be adopted for the columns.

This paper presents a preliminary numerical investigation on column shear failure due to local interaction between structural and non-structural elements, generally defined as "*local shear interaction*". The starting point for this research work are the results of some experimental tests on infilled RC frames performed by the Authors (Verderame et al., 2016). Two conforming and non-conforming infilled frames were tested, designed according to the current Italian seismic technical code (SLD), and according to an older Italian technical code in order to be representative of existing RC buildings constructed between 1970s and 1990s (GLD). Infill panels were made of hollow clay bricks, common in Mediterranean countries. Due to the differences in these two

specimens, the GLD frame exhibited a column shear failure due to interaction with the infill; on the contrary, in SLD frame no shear failures were experimentally detected. Different strategies of macro-modelling for infills and different shear strength models are applied and discussed, in order (i) to match the experimental response in terms of initial stiffness, peak strength and corresponding displacement, and softening behaviour and (ii) to capture (or not) the column shear failure exhibited (or not) during the test. The best modelling strategy is finally identified to provide a support towards further numerical investigations.

2 LOCAL SHEAR INTERACTION MODELLING FROM LITERATURE

Experimental data about infilled RC frames have been the support for analytical modelling efforts since late 1970s'. Infills have been generally modelled by means of quite complex FEM micro-modelling approaches or simpler single- or multi-struts (reacting only in compression) approaches. Nevertheless, even recently, there is lack of unanimity about the best modelling approach among the various literature proposals (e.g., Chrysostomou et al. 2002; Ricci et al. 2016; De Risi et al. 2018), above all about the column-infill shear interaction modelling strategy, since, obviously, the shear demand in the surrounding RC members strictly depends on the modelling strategy to reproduce the infill response.

2.1 Definition of the shear demand in columns

More specifically, about the shear failure modelling in non-ductile RC frames, some standards propose simplified procedures aimed at taking into account the effects of the interaction between infill panels and surrounding RC elements. These procedures usually consider a concentrated load on the column (or beam) equal to the horizontal (or vertical) component of the resultant of the stresses along the loaded diagonal of the infill panel.

Among codes, some practice-oriented prescriptions are present in the American code ASCE/SEI 41-06 (2007), which suggested to model the infill as a single eccentric strut in compression as shown in Figure 1a. On the contrary, the most recent Italian technical standards (D.M. 2008; D.M. 2018) do not provide any suggestion for the modelling and the assessment of the local interaction phenomena in the case of solid panels adjacent to column/beam elements.

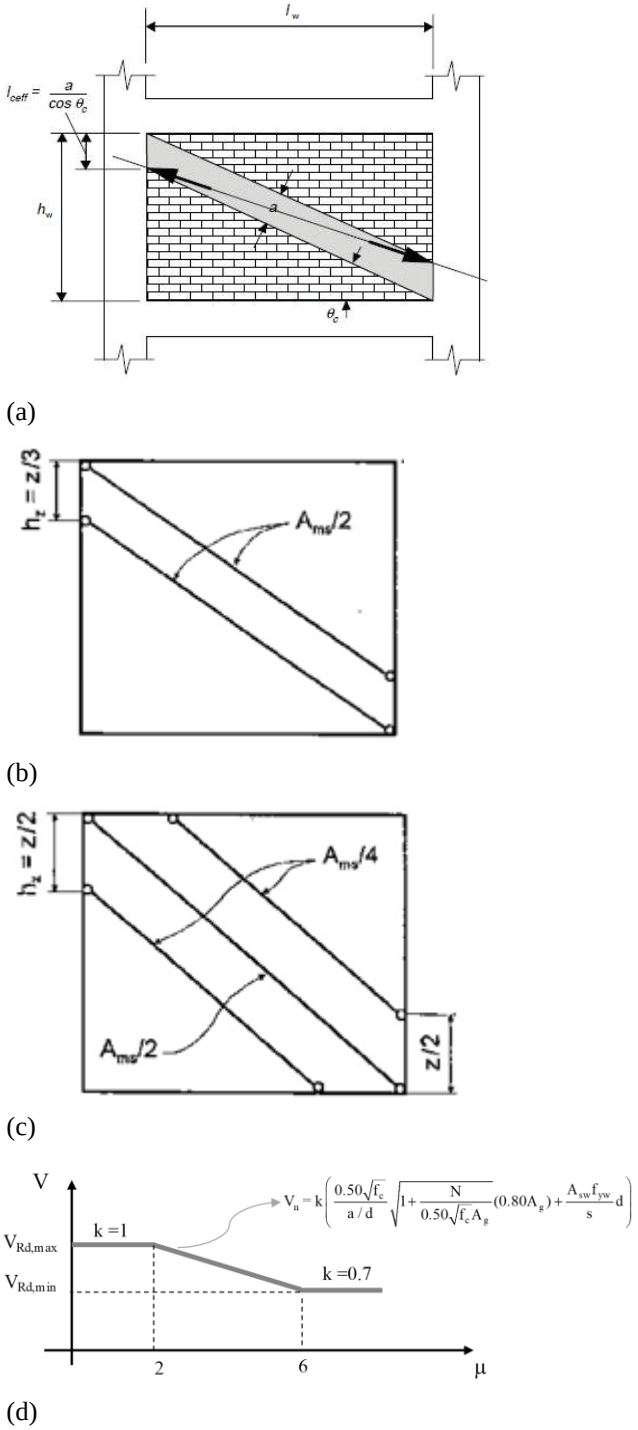

Figure 1. Examples of single eccentric strut (a), and two- (b) or three- (c) struts modelling approaches suggested in literature (ASCE-SEI/41, 2007; Crisafulli et al., 1997); shear strength model by Sezen and Moehle (2004).

About research studies from literature, the issue of shear failure modelling in non-ductile RC frames due to local interaction with infill elements has been investigated with different approaches (Figure 1) during the last years (e.g., Crisafulli 1997; Burton and Dierlein 2014; Sattar and Liel 2015; Jeon et al. 2015; among others). Multiple-strut approaches are often suggested in these studies, generally proposing to model the infill by a minimum of one-strut - eccentrically placed with respect to the infill diagonal, like suggested in the

ASCE-SEI/41 (2007) - to a maximum of two (Figure 1b) or three struts (Figure 1c), basically different for the position of the loading points on the adjacent columns, the ratio of the total infill lateral load adsorbed by each strut, and for the struts inclination. The number of struts, their positions, and their width have to be carefully selected to reliably reproduce the stress demand they induce and the strength and deformability contribution of the panel to the infilled RC frame.

2.2 Assessment of the column shear capacity

A key issue for the shear local interaction modelling is the adequacy and the applicability of the usually adopted shear capacity models in capturing the shear-controlled behaviour of a RC member adjacent to an infill panel.

All the proposals from codes and literature mentioned above suggest to use the model by Sezen and Moehle (2004), also adopted in the American code ASCE-SEI/41 (2017), as shown in Figure 1d. This model assumes a shear strength degradation due to the inelastic ductility demand, as typical in mono-dimensional columns/beams. In the case of very "squat" portions of columns, as those generated by the limited infill-to-column contact length (as shown in Figure 1a-c), a shear strength degradation due to an increasing flexural demand appears not totally meaningful. Therefore, the model by Sezen and Moehle (2004) should be applied without any strength degradation (k=1 in Figure 1d). Alternatively, a different "family" of shear strength models should be adopted, degrading with the shear crack opening demand or, from a predictive standpoint, with the strain demand, instead than with the flexural inelastic ductility demand, as suggested in the following sections.

3 INFILL MODELLING PROPOSAL

The infilled frames have been modelled as shown in Figure 2. The considered loading direction is shown with a red arrow in these figures. However, if the opposite loading direction is considered, all the remarks reported in the following text can be repeated in a specular way. Increasing horizontal displacements are imposed faithfully reproducing the experimental setup used during the tests analysed later.

The fibre-type *ForceBeamColumn* element has been adopted in OpenSees (McKenna et al., 2010) for each beam/column element. Mander et al. (1988)'s concrete law, considering confining effect, if any, has been used (*Concrete04 uniaxial material*). *ReinforcingSteel uniaxial material* reproduces the experimental constitutive laws of the reinforcing steel. Beams and columns have been considered as ductile members. Beam-column joints are considered as supplied by infinite strength and stiffness.

The modelling of infills adopted herein is based on two strategies.

The first one models the infill as a single compressive diagonal strut (as shown in Figure 2a). Such an approach is generally adopted to catch the global behaviour of infilled frames, being able to reproduce the contribution of the infill panel to the global strength and stiffness of the infilled frame. In this case, the horizontal response of the infill is simply projected along the diagonal direction to characterise the axial load-deformation behaviour of the compressive strut.

Nevertheless, this model is not able to detect any eventual localised shear demand in the surrounding RC members, thus failing in the detection of eventual shear failures of the adjacent columns induced by the infill-column shear interaction. Therefore, the second modelling approach reproduces the infill contribution by means of three parallel compressive struts (as shown in Figure 2b) based on the proposals by Chrysostomou et al. (2002) and Jeon et al. (2015). First, the contact length z between infill panel and column is computed by following the approach proposed by Stafford Smith (1963). In the critical section of column shear failure, assumed to be located at a distance equal to the column effective depth from the beam-column interface (Jeon et al., 2015), the contact length z is divided into two portions: one in contact with the lower part of the central strut and the other in contact with the lower off-diagonal strut. The portion of the global lateral load absorbed by the central strut (γ_c) is determined based on the corresponding area of the bearing stress distribution with respect to the total area of the same bearing stress distribution, according to the proposal by Jeon et al. (2015). On the same bases, the end-point of the lower off-diagonal truss (z_c in Figure 2b) is obtained.

Additionally, elastic stiffness, secant-to-peak stiffness and lateral loads of the off-diagonal struts are reproduced according to the proposal by Chrysostomou et al. (2002), depending on their eccentricity with respect to central diagonal strut, and, more specifically, depending on the parameter $\alpha = (z_c / H_w) < 1$ (where H_w represents the infill panel height, as shown in Figure 2b).

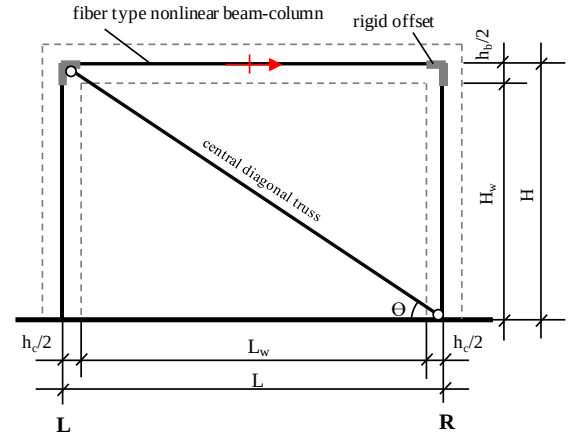

(a)

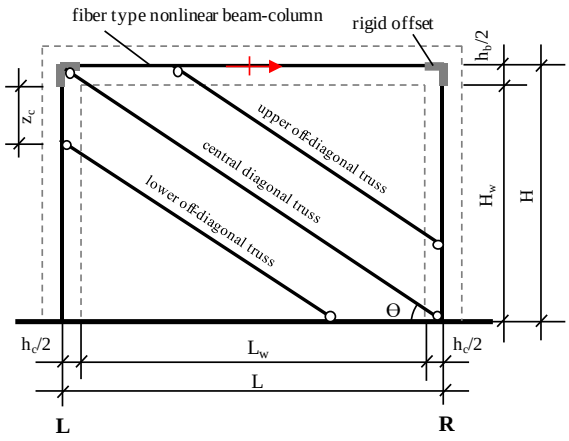

(b)

Figure 2. Single concentric- (a) and three- (b) strut modelling approaches adopted herein.

First, being K and ΔU the global stiffness of the infill panel and an assigned incremental displacement in horizontal direction, respectively, the axial stiffness of the central diagonal strut (k_c) and related incremental displacement (Δu_c) can be computed as in Eqs. (1) and (2):

$$k_c = \frac{K}{\cos^2\theta}\cdot\gamma_c \quad (1)$$

$$\Delta u_c = \Delta U\cdot\cos\theta \quad (2)$$

Axial stiffness of the off-diagonal struts (k_{off}) and related incremental displacement (Δu_{off}) can be obtained in the hypothesis of linear deformed shape of the columns, as suggested by Chrysostomou et al. (2002) and shown in Eqs. (3) and (4):

$$k_{off} = \frac{K - k_c\cdot\cos^2\theta}{2(1-\alpha)^2\cdot\cos^2\theta} = \frac{K(1-\gamma_c)}{2(1-\alpha)^2\cdot\cos^2\theta} \quad (3)$$

$$\Delta u_{off} = \Delta U\cdot\cos\theta\cdot(1-\alpha) \quad (4)$$

The same eccentricity parameter and lateral load-portion has been assumed for the two off-diagonal struts, for the sake of simplicity. As a result, the incremental axial load acting in the central diagonal and off-diagonal struts can be calculated, as the product between the axial stiffness and related incremental displacement.

Furthermore, in order to avoid introducing further variables to the modelling approach used herein, the global infill constitutive relationship adopted for numerical simulations in terms of horizontal load (V_w)- versus- horizontal displacement (D) (or, equivalently, drift) will be obtained from the experimental responses analysed later. The latter will be derived as the difference between the experimental responses of the infilled frame and the corresponding bare one, thus assuming that the RC frame and the infill panel work as a parallel system (as in De Risi et al., 2018).

4 DETECTION OF SHEAR FAILURE

The three-struts numerical model described above can provide the shear demand acting on the columns, but it does not explicitly account for potential columns shear failures.

Shear failures in columns can be first detected starting from a post-processing of the numerical output, but a proper shear strength model should be selected, suitable for squat columns, as those generated by the column-to-infill interaction. Therefore, two models have been adopted herein as explained in the following.

First, shear strength is evaluated according to ASCE/SEI 41 (2017) (see Eq. (5)), as proposed by Sezen and Moehle (2004) ("S&M") and very commonly adopted in previous studies from literature for similar applications.

$$V_n = k\left(\frac{0.50\sqrt{f_c}}{a/d}\sqrt{1+\frac{N}{0.50\sqrt{f_c}A_g}}(0.80A_g)+\frac{A_{sw}f_{yw}}{s}d\right) \quad (5)$$

where a/d is the shear span-to column effective depth ratio, A_g the gross area of the column, A_{sw}, f_{yw}, and s are the transverse reinforcement area, yielding strength and stirrups spacing, respectively. N is the column axial load at the interface section with the joint and changes for increasing applied horizontal displacement (reaching a minimum value in the left column and a maximum value in the right column, given the assumed loading direction in Figure 2). Actually, ASCE/SEI 41 (2017) suggests to conservatively assume N=0 in Eq. (5) to assess the shear capacity in columns subjected to the local shear interaction with the surrounding infills. Such an assumption can result too much conservative for the numerical-versus-experimental comparison. Therefore, the actual axial load acting on the column (and varying step-by-step) is assumed herein in Eq. (5). The coefficient k takes into

account the strength degradation due to the inelastic ductility demand. Since the lack of meaning of a strength degradation assessment due to an increasing flexural demand in such a squat columns, the strength model by ASCE/SEI-41 (2017) is applied herein always by imposing k=1. The shear span a in Eq. (5) has been assumed as equal to the distance between the null point of the moment diagram in the squat portion of column and the beam-column interface (variable during the analysis), limiting the a-to-d ratio between 2 and 4, as prescribed by Sezen and Moehle (2004) and in ASCE/SEI-41 (2017).

Additionally, as anticipated in Section 2.2, a different "family" of shear models could be adopted for the squat columns of the infilled frames. A model providing a strength value that degrades with the crack opening demand or, from a predictive standpoint, with the strain demand (numerically evaluable) - instead than with the flexural inelastic ductility demand - should be more suitable for the very "squat" portions of columns due to the limited infill-to-column contact length. Therefore, the modified compression field theory (MCFT) model (Vecchio and Collins, 1986) has been analysed and, in particular, its more practical simplification (Bentz et al., 2006) is adopted herein. According to the Simplified MCFT (SMCFT) proposed by Bentz et al. (2006), shear strength can be evaluated according to Eq. (6):

$$V_{Rd} = \beta\sqrt{f_c}(b_w \cdot d) + \frac{A_{sw} f_{yw}}{s} \cdot 0.9d \cdot \cot\theta \qquad (6)$$

where coefficient β represents the capacity of cracked concrete to transfer shear stress, and Θ is the inclination of the principal compressive stress. Both β and Θ depend on the shear crack opening demand, namely, on the longitudinal strain demand (ε_x) (see Bentz et al., 2006). The longitudinal strain at the mid-depth of the web (ε_x) is evaluated as equal to one-half of the strain in the longitudinal tensile reinforcing steel (Bentz et al., 2006) in a "critical section" located at a distance d from the null point of the bending moment (see Figure 3), also taking into account the translation of the bending moment diagram, as suggested by Model Code (2010), namely:

$$\varepsilon_x = \frac{1}{2A_s E_s} \cdot \left(\frac{M}{d^*} + V - 0.5N \right) \qquad (7)$$

where A_s and E_s are tensile longitudinal steel area and Young modulus of steel, respectively; V, M and N represent the shear, moment and axial compression demand, respectively, acting on the (squat) column at the "critical section" (see Figure 3), and d^* is assumed equal to 0.9 times the effective depth of the column. Therefore, a shear failure is detected if the column shear demand-drift curve intersects the column shear capacity-drift curve, for a shear value hereinafter referred to as $V_{col,SF}$.

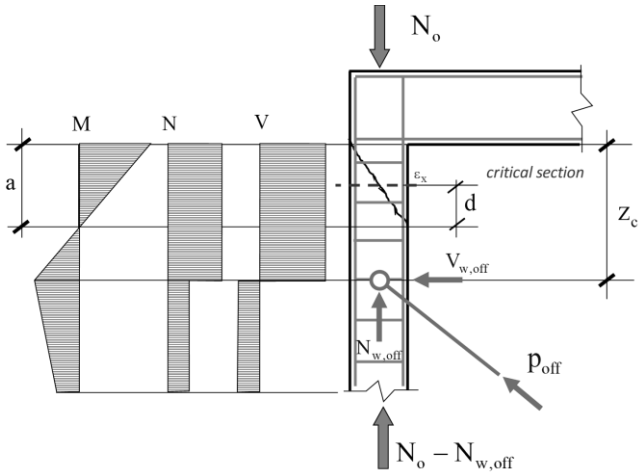

Figure 3. Definition of the critical section for shear safety check.

The shear failure could be also directly detected by properly adding to the numerical model shown in Figure 2b an explicit shear spring in the squat column, as shown in Figure 4a. This spring could be defined by means of a sort of "limit state material" (as defined in Elwood, 2004), which monitors the strain demand in the critical section of the column (according to Bentz et al., 2006) instead of the inter-story drift demand (as originally suggested by Elwood, 2004) during the analysis. Such a monitoring possibility is currently not implemented in OpenSees platform; therefore, herein, the strength of this spring is defined as the shear demand for which the shear failure is achieved ($V_{col,SF}$).

The shear spring introduced in the model is characterized by an elastic stiffness up to $V_{col,SF}$, and by a softening constant stiffness up to a residual strength ($V_{c,res}$), if any (see Figure 4b). The softening stiffness adopted is defined according to Elwood and Moehle (2005) proposal (referred to as "E&M" in the following). On a mechanical base, Elwood and Moehle (2005) proposed to estimate the displacement $\delta_{a,E\&M}$ at which a column begins losing its axial load carrying capacity after the occurrence of a shear failure as in the equation reported in Figure 4b, (where L is imposed equal to z_c, thus defining the displacement $\delta_{a,E\&M}$ as the relative displacement between the two ends of the squat column). Additionally, the column axial load N is assumed equal to its initial value (N_0). Such a displacement

coincides with the total loss of lateral load carrying capacity ($V_{c,res}$=0).

Additionally, the shear critical angle θ in Eq. suggested by Elwood and Moehle (2005) is equal to 65°. Nevertheless, the values of θ should be coherent with that used in Eq. (6) (θ_{SMCFT}). Therefore, both these values of θ have been used for sake of comparison in the following analyses: the one suggested by Elwood and Moehle (2005) and θ_{SMCFT}.

In both cases, the shear spring has been introduced in the numerical model in OpenSees as shown in in Figure 4, namely by means of a *ZeroLength Element* (between two nodes, in red, geometrically coincident) defined with a *Hysteretic Uniaxial Material*.

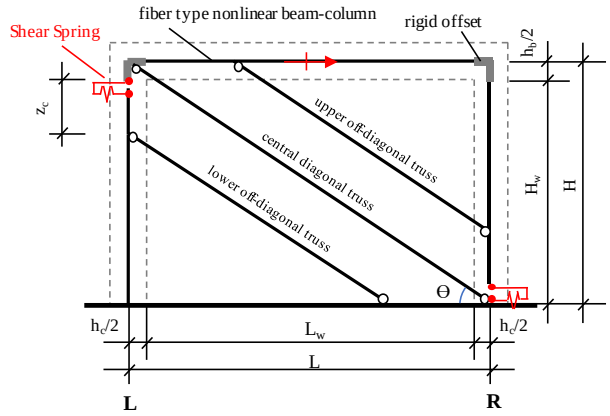

(a)

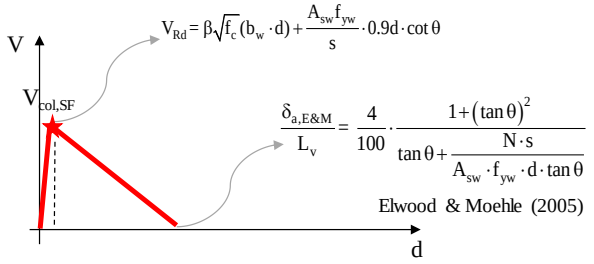

(b)

Figure 4. Shear spring explicit modelling (a) and backbone (b).

5 PRELIMINARY VALIDATION BY MEANS OF EXPERIMENTAL DATA

Two one-storey one-bay half-scaled RC frames (shown in Figure 5) were tested and presented in Verderame et al. (2016). One frame was non-conforming and the other was conforming to the most updated seismic code provisions. These specimens represent the preliminary test-bed of the modelling strategies presented in this paper. Their main results are very briefly recalled in Section 5.1.

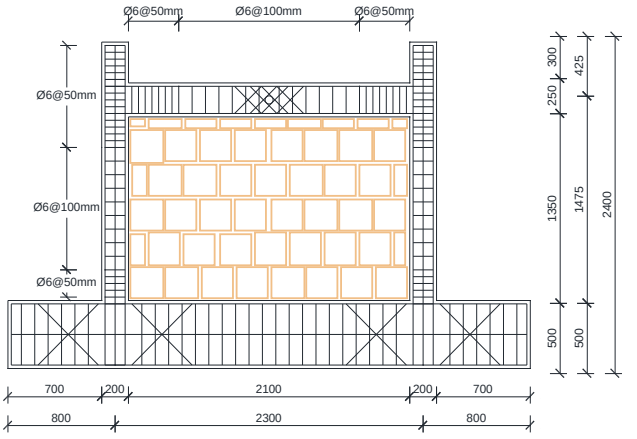

(a)

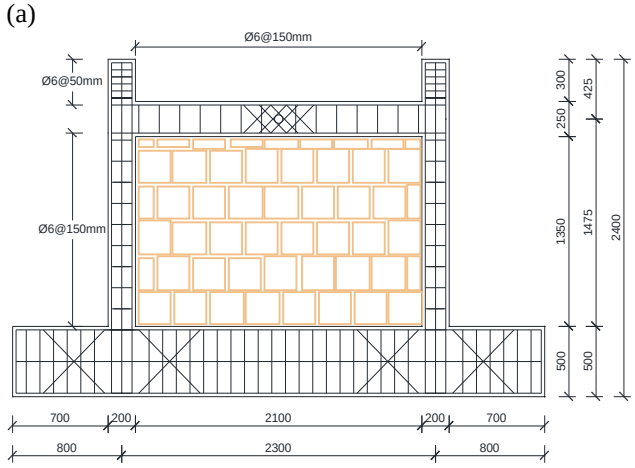

(b)

Figure 5. SLD (a) and GLD (b) frames tested by Verderame et al. (2016)

5.1 Analysed experimental data

The non-conforming frame (Figure 5a) analysed herein was designed for gravity loads only (GLD) and infilled with 80 mm thickness hollow clay bricks. Hereinafter it will be referred to as GI-80. It was representative of the bottom storey of a five-storey gravity load designed RC frame, according to Italian technical codes in force between 1970s and 1990s (D.M. 72; D.M. 92).

The conforming specimen (Figure 5b) was designed for seismic loads (SLD) and infilled as the GI-80 specimen. Hereinafter it will be referred to as SI-80. It was designed according to the Italian seismic code D.M. 2008, in compliance with all the capacity design requirements.

Mean value of 28-day cylindrical concrete strength was equal to 21.9 MPa. Deformed bars of the commercial typology of reinforcing steel B450C were used, characterized by a mean yielding strength equal to 507 MPa, 586 MPa, 490 MPa and 481 MPa, for bar diameters of 6 mm, 8 mm, 10 mm, and 12 mm, respectively. Hollow clay units with cement mortar were used as infill material. Dimensions of brick units were

250×250×80 mm^3. The mortar had a mean compressive strength of 14.03 MPa. Additional details about reinforcement and material properties can be found in Verderame et al. (2016).

About the test setup, the lateral load was applied by means of a hydraulic actuator in displacement control. The actuator was fixed to a steel reaction wall. The actuator was connected to the mid-span of the beam through steel profiles connected to steel rod passing through the transverse hole in the mid-span of the beam. The related loading protocol applied to the infilled specimens consisted of 3-push-pull-cycles per each imposed drift levels, the latter assumed to be equal to 0.01%, 0.02%, 0.15%, 0.50%, 0.90%, 1.30%, 1.70%, 2.00%, 2.40%, 3.00%, and 3.6%. The vertical load on columns was applied by hydraulic jacks in load control and it was kept constant during the tests and corresponding to an axial load ratio equal to 10%. The lateral load-top drift responses for these two specimens are shown in Figure 6.

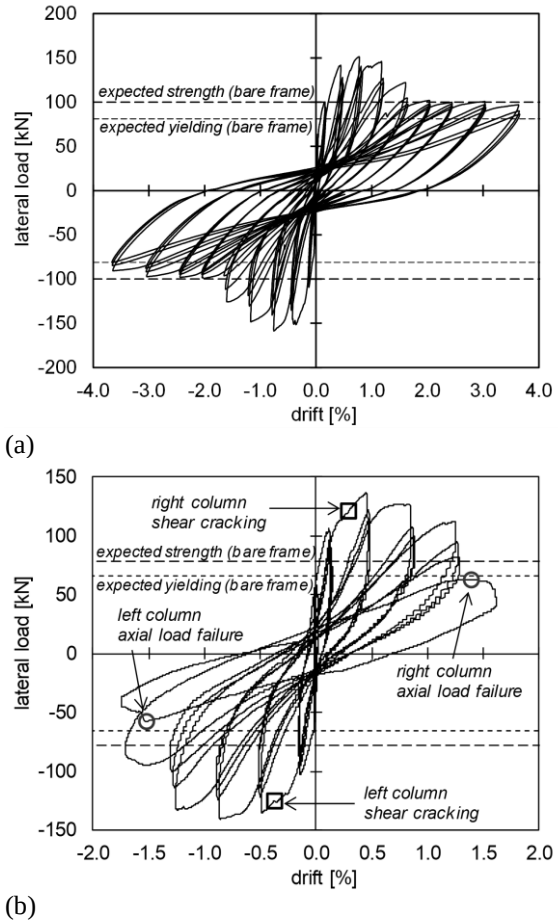

Figure 6. Global responses for SI-80 (a) and GI-80 (b) specimens – adapted from Verderame et al. (2016).

In summary, a ductile, flexure-controlled post-elastic behaviour of the frame, without shear failures in RC members, was observed for SI-80 specimen. The formation of a plastic mechanism involving beam's ends and columns' base was observed. A corner crushing failure of the infill, completed at the peak load of the response, occurred.

For GI-80 specimen, diagonal cracking developed in the panel since very low drift values (i.e., between 0.15% and 0.50%). A drop in lateral force associated to the development of severe diagonal cracking at the top of the columns (with crack inclination quite close to 45°) was observed for an applied drift range between 0.50% and 1.30%. At 1.70% of drift, an abrupt increase in vertical displacement of the top of the columns also occurred, highlighting the potential for an imminent axial failure. The observation of the local behaviour showed the evidence of a shear failure due to the local interaction between RC columns and infill panel, as also marked on the cyclic response of the specimen in Figure 6b.

5.2 Numerical versus experimental comparisons

The results of the described modelling approach explained in Section 3, with a single- (dotted red line) or a three-strut (solid red line) infill model, are shown in Figure 7a and Figure 7b for test SI-80 and GI-80, respectively. Note that V_b in Figure 7 is the base shear, which coincides with the applied lateral load. In both cases, the global infill constitutive relationship adopted for numerical simulations in terms of horizontal load (V_w)-drift has been obtained from the experimental responses, as described in De Risi et al. (2018). Additionally, as a result of the application of Jeon et al. (2015) and Chrysostomou et al. (2002) suggestions recalled in Section 3, for the three-struts model, the central diagonal truss absorbs 35% of the global lateral load (γ_c = 0.35); for the off-diagonal struts, $\gamma_{off\text{-}diagonal}$ = 0.33.

The numerical- versus- experimental comparison for the SI-80 frame (Figure 7a) shows a very good matching in terms of maximum load and also initial stiffness and frame deformability in the first loading steps. The maximum lateral load finally achieved during the simulation is equal to 159.0 kN, very close to the corresponding experimental value (-158.6 kN). Moreover, at about 2.00% drift, lateral load drops up to the predicted flexural strength (V_{max}) of the bare frame only, in tune with the experimental evidence.

Regarding the test GI-80 (see Figure 7b), the agreement between modelling results and experimental findings appears very good in terms of maximum load and also initial stiffness and

frame deformability, especially in the ascending branch of the lateral behaviour up to shear cracks in the column start to significantly increase their width (namely until the penultimate cycle of the response). The maximum lateral load achieved during the simulation is equal to 140.9 kN, that is very close to the corresponding experimental value (-140.1 kN).

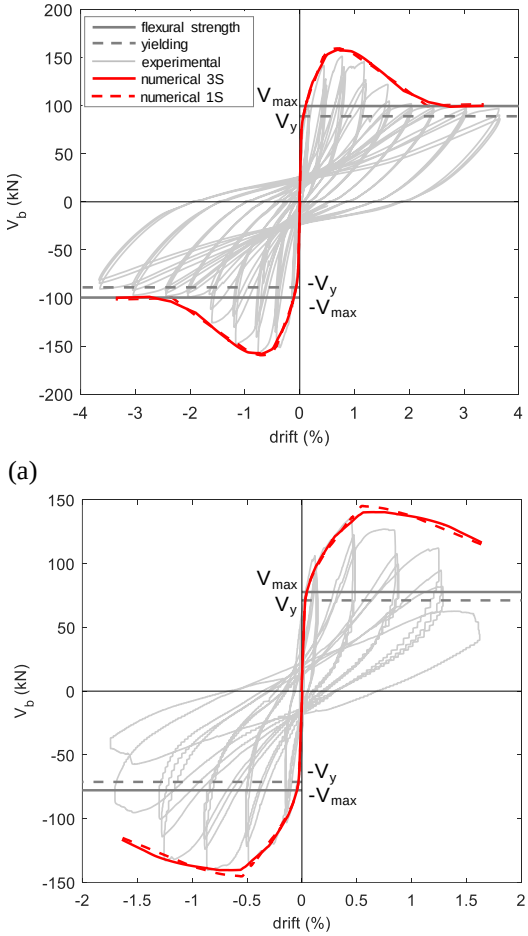

Figure 7. Numerical (red) versus experimental (grey) response: test SI-80 (a); test GI-80 (b) single-strut (dotted red line) and tri-strut (solid red line) modelling approaches.

The eventual column shear failures are first checked by means of a post-processing of the analysis results (as explained in Section 4). In particular, the attention will be focused on the left (L) side column, where axial load decreases during the simulation thus producing a reduction in shear strength, and which clearly reached the cracking condition during the test GI-80 (where local shear interaction exhibited the most significant experimental evidence), according to Verderame et al. (2016). Both shear strength models, by ASCE/SEI 41 (2017) and by Bentz et al. (2006) (SMCFT) are applied herein for both the infilled specimens (see Figure 8). As a result, for SI-80 specimen, no column shear failure is detected, since shear strength capacity evaluated by both SMCFT theory and "S&M" proposal is higher than the maximum column shear demand (see Figure 8a). Additionally, no shear failure has been detected by ASCE/SEI 41's strength model (with k=1) for GI-80 specimen (see "S&M" curve in Figure 8b). Note that V_{Rd} by "S&M" model is reducing for increasing drift levels due to the action of the lower off-diagonal strut that produces a progressive reduction of the column axial load. On the contrary, for test GI-80, Bentz et al. (2006)'s proposal leads to a column shear failure at about 1.0 % of applied lateral drift (red star in Figure 8b), namely on the descending branch of the global lateral response (red curve), as experimentally observed. $V_{col,SF}$ is equal to 52.4 kN in this case. Note that Figure 8 also shows axial load (N) and shear demand (V) variation during the simulation (in grey and black solid line, respectively), together with the global (V_b-drift) response (red line).

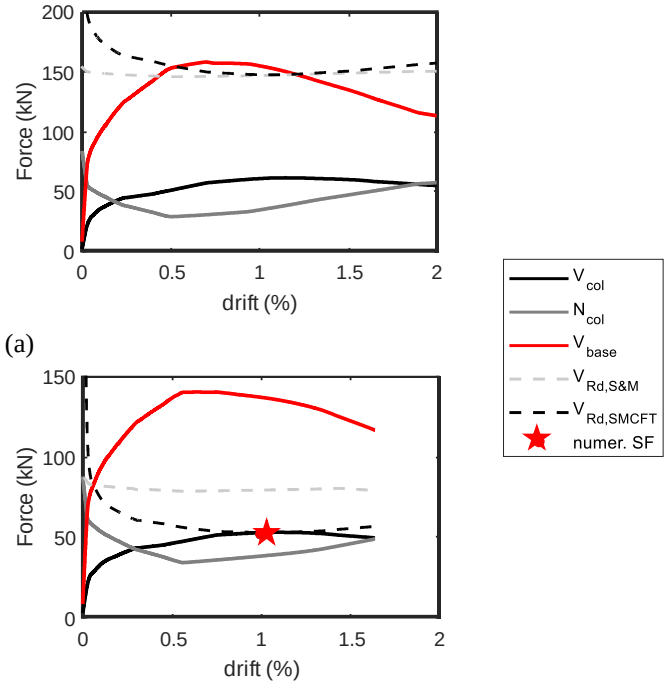

Figure 8. Shear failure (SF) detection for left-side squat column for test SI-80 (a) and GI-80 (b).

In a second step of modelling, for the specimen GI-80, where the shear failure is detected by the application of the SMCFT model, an explicit shear spring has been added to the model, as shown in Figure 4a and explained in Section 4. Such a spring is linear elastic up to $V_{col,SF}$, and then characterised by a softening constant stiffness up to a null residual strength ($V_{c,res}$ = 0). The softening stiffness adopted is defined according to Elwood and Moehle (2005) proposal, where the shear critical angle θ should be first defined. If θ is

evaluated according to the SMCFT at the onset of the shear failure (θ_{SMCFT}), the value of 41.2° is obtained. Otherwise, according to Elwood and Moehle (2005) proposal, θ is equal to 65°. Both these hypotheses on θ (65° and 41.2°) have been analysed and compared. The corresponding values of $\delta_{a,E\&M}$ are equal to 30 mm and 8.2 mm, respectively. Note that the θ_{SMCFT} value is closer to the experimental main shear crack angle reported in Verderame et al. (2016). Therefore, a better prediction of the numerical response is expected when $\delta_{a,E\&M}$ is evaluated with $\theta = \theta_{SMCFT}$.

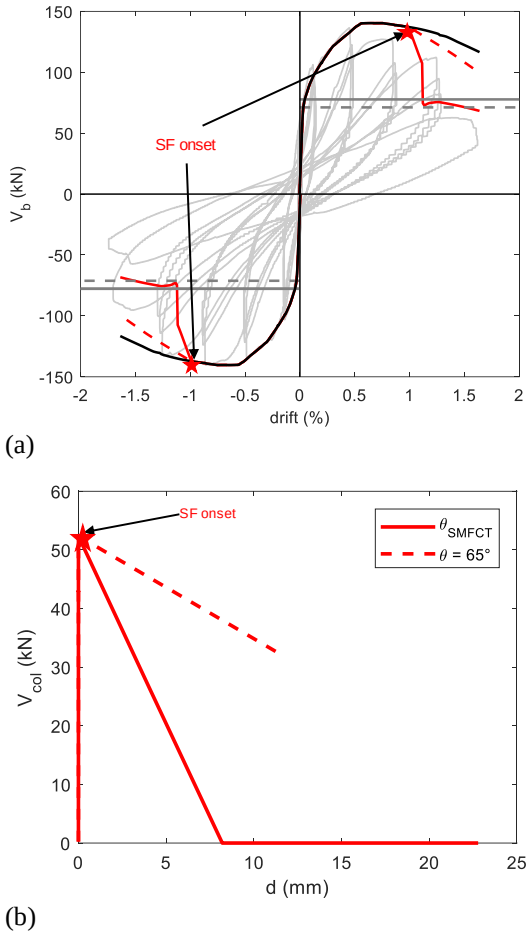

Figure 9. Numerical-versus-experimental comparison for test GI-80 including column shear spring with θ_{SMCFT} (solid red line) or θ=65° (dotted red line) (black line is related to the simulation without shear spring) (a); shear spring responses depending on the value of θ (b).

The results of these simulations for the specimen GI-80 are shown in Figure 9a and the related responses of the shear spring are reported in Figure 9b. It can be observed that shear failure – meant as the initiation of a shear-controlled softening response – begins at a drift value roughly equal to 1% (see Figure 9a). The global softening branch changes depending on the assumption adopted for θ. The numerical response better reproduces the experimental response if the θ_{SMCFT} value is adopted (red solid lines in Figure 9a).

6 CONCLUSIONS

A preliminary numerical investigation on column shear failure due to local interaction between structural and masonry infill elements has been presented, starting from the results of some experimental tests on infilled frames performed by the Authors (Verderame et al., 2016). Different shear strength models and different strategies of macro-modelling for infills have been applied and discussed, in order to (i) capture (or not) the column shear failure exhibited (or not) during the test and (ii) to match the experimental response in terms of initial stiffness, peak strength and corresponding displacement, and softening behaviour. The analysed experimental data have been briefly described and numerically reproduced by means of proper models carefully taking into account the local shear interaction between infill panel and RC columns observed during one of the analysed tests.

It resulted that the shear demand on the surrounding columns due to the interaction with the infill panels could be well caught by means of a three-compressive struts modelling approach, properly identifying the location and the contribution of each strut according to the proposals by Jeon et al. (2015) and Chrysostomou et al. (2002).

On the other side, the column shear strength could be well estimated based on the modified compression field theory (Bentz et al., 2006), a model more suitable for the squat columns produced by this interaction with respect to shear strength models degrading due to the increasing cyclic inelastic flexural demand.

The numerical results shown in the paper appear to be very close to the experimental ones. Nevertheless, further efforts will be devoted to the extension of this modelling strategy to other similar specimens experimentally tested in the literature, to finally provide a wider validation of the proposed modelling approach.

ACKNOWLEDGEMENTS

This work was developed under the support of the AXA Research Fund Post-Doctoral Grant "Advanced nonlinear modelling and performance assessment of masonry infills in RC buildings under seismic loads: the way forward to design or retrofitting strategies and reduction of losses" funded by AXA Research Fund and ReLUIS-DPC 2019-2021 funded by the Italian Department of

Civil Protection (DPC). These supports are gratefully acknowledged.

REFERENCES

Mehrabi, A.B., Shing, P.B., Schuller, M.P., Noland, J.L., 1996. Experimental evaluation of masonry-infilled RC frames. *Journal of Structural Engineering*, **122**(3), 228-237.

Al-Chaar, G., Issa, M., Sweeney, S., 2002. Behavior of masonry-infilled non-ductile reinforced concrete frames. *Journal of Structural Engineering*, **128**(8), 1055-1063.

Chrysostomou, C.Z., Asteris, P.G., 2012. On the in-plane properties and capacities of infilled frames. *Engineering Structures*, **41**, 385-402.

Ricci, P., De Risi, M.T., Verderame, G.M., Manfredi, G., 2016. Procedures for calibration of linear models for damage limitation in design of masonry-infilled RC frames. *Earthquake Engineering and Structural Dynamics*, **45**(8), 1315-1335.

De Risi, M.T., Del Gaudio, C., Ricci, P., Verderame, G.M., 20018. In-plane behaviour and damage assessment of masonry in-fills with hollow clay bricks in RC frames. *Engineering Structures* **168**:257–275.

ASCE/SEI 41-06. Seismic rehabilitation of existing buildings. American Society of Civil Engineers, Reston, VA, USA, 2007.

D.M. 2008, D.M. 14/01/2008. Approvazione delle nuove norme tecniche per le costruzioni. G.U. n. 29 del 4/2/2008. (in Italian)

D.M. 2018, D.M. 17/01/2018. Aggiornamento delle nuove norme tecniche per le costruzioni. G.U. n. 42 del 20/2/2018. (in Italian)

Crisafulli, F. J., 1997. *Seismic behaviour of reinforced concrete structures with masonry infills*, PhD Thesis, University of Canterbury, New Zealand.

Burton, H., Deierlein, G., 2014. Simulation of seismic collapse in non-ductile reinforced concrete frame buildings with masonry infills. *Journal of Structural Engineering*, 140 (SI: Computational simulation in structural engineering). **140**(8), A4014016.

Sattar, S., Liel., A.B., 2015. Seismic performance of nonductile reinforced concrete frames with masonry infill walls: I. Development of a strut model enhanced by finite element models. *Earthquake Spectra*, **32**(2), 795-818.

Jeon, J.S., Park, J.H., DesRoches, R., 2015. Seismic fragility of lightly reinforced concrete frames with masonry infills. *Earthquake Engineering and Structural Dynamics*, **44**(11), 1783-1803.

Sezen, H., Moehle, J.P., 2004. Shear Strength Model for Lightly Reinforced Concrete Columns. *Journal of Structural Engineering*, Vol. **130**, No. 11.

ASCE/SEI 41, Seismic evaluation and retrofit of existing buildings. American Society of Civil Engineers, Reston, VA, USA, 2017.

McKenna, F., Fenves, G.L., Scott., M.H., 2010. OpenSees: Open System for Earthquake Engineering Simulation. Pacific Earthquake Engineering Research Center. University of California, Berkeley, CA, USA. http://opensees.berkeley.edu.

Mander, J.B., Priestley, M.J.N., Park, R., 1988. Theoretical stress-strain model for confined concrete. *Journal of Structural Engineering*, **114**(8), 1804-1826.

Stafford Smith, B., 1963. Lateral stiffness of infilled frames. *J Struct Div, ASCE*; **88** (ST6):183–99.

Vecchio, F. J., Collins, M.P., 1986. The modified compression-field theory for reinforced concrete elements subjected to shear. *ACI J.*, **83**(2), 219-231.

Bentz, E. C., Vecchio, F.J., Collins, M.P., 2006. Simplified modified compression field theory for calculating shear strength of reinforced concrete elements. *ACI Materials Journal*, **103**(4), 614.

Model Code 2010-first complete draft. Fédération Internationale du Béton fib/International Federation for Structural Concrete, 2010.

Elwood, K.J., 2004. Modelling failures in existing reinforced concrete columns. *Canadian Journal of Civil Engineering* **31**(5):846–859.

D.M. 30/05/1972 Norme tecniche alle quali devono uniformarsi le costruzioni in conglomerato cementizio, normale e precompresso ed a struttura metallica. alla G.U. n. 190 de 22/7/1972. (in Italian)

D.M. 14/02/1992. Norme tecniche per l'esecuzione delle opere in cemento armato normale e precompresso e per le strutture metalliche. Suppl. Ord. alla G.U. n. 65 del 18/3/1992. (in Italian)

Verderame, G. M., Ricci, P., Del Gaudio, C., De Risi, M.T., 2016. Experimental tests on masonry infilled gravity-and seismic-load designed RC frames. In *Brick and Block Masonry: Trends, Innovations and Challenges-Proceedings of the 16th International Brick and Block Masonry Conference, IBMAC* (pp. 1349-1358), June 2016, Padova, Italy.